International journal of basic and applied research
www.pragatipublication.com
ISSN 2249-3352 (P) 2278-0505 (E)
Cosmos Impact Factor-5.86

EFFECT OF PVA CONCENTRATION ON STRUCTURAL, MORPHOLOGICAL, OPTICAL AND ELECTRICAL PROPERTIES OF PVA CAPPED SnS NANOCRYSTALLINE FILMS GROWN BY CHEMICAL BATH DEPOSITION

POTNURU MOHANKRISHNA, VELAGA SURYAKALA, GADU RAMBABU, DASARI TIRUMALA RAO
Assistant Professor[1,2,3] Associate Professor[4]
Sri Venkateswara College of Engineering & Technology,
Etcherla,Srikakulam,Andhra Pradesh-532410
Department of ECE

ABSTRACT
Chemical bath deposition (CBD), a straightforward and inexpensive wet chemical method, has been used to effectively produce nanocrystalline films of polyvinyl alcohol (PVA) capped tin monosulfide (SnS) on glass substrates. The concentrations of PVA used ranged from 0.5 wt % to 2 wt %. The XRD analysis showed that the SnS phase is best represented by peaks with an orientation of (040). The use of XRD spectra allowed for the estimation of many characteristics, including stacking faults, dislocation density, lattice strain, and average crystallite size. The XRD findings were further validated by Raman analysis. The films deposited at a 2 wt % concentration of PVA showed acceptable morphology in the SEM and AFM micrographs. FTIR analysis confirmed that the films contained PVA. The experimental films' high absorbing nature was corroborated by the optical examinations, which also revealed a blue shift in band gap values with increasing PVA concentration. As a result of the quantum confinement effect, the predicted band gap values range from 1.73 eV to 1.55 eV. All of the developed layers exhibited p-type conductivity, according to Hall measurement tests. We also talk about the findings from our study on the effects of different PVA concentrations on electrical resistivity, carrier concentration, and mobility.
Chemical Bath Deposition, Polyvinyl Alcohol, Structural Properties, Optical Properties, and Morphological Properties are the keywords here.

1. INTRODUCTION

2. Research into the creation of photovoltaic devices via the use of novel technology, materials, and methods has recently garnered a lot of interest due to the fact that these advancements result in decreased costs and improved efficiency. To create different types of semiconductor nanocrystalline layers for use in devices, one processing step is to use polymer matrices as a capping agent. It is possible to modify the physical behavior, especially the electrical and optical characteristics, by covering the layers of semiconductors with polymers. Solar cells, field effect transistors, electroluminescence devices, and light-emitting diodes all rely on their size and shape regulation capabilities, making them very important [1–5]. The particle size is reduced and the surface to volume ratio is increased by capping. Many scientists have come to trust polyvinyl alcohol (PVA) as a viable capping agent and have found it useful in nano production among other organic materials. This is mostly because of its many desirable properties, such as being chemically resistant, transparent throughout the visible spectrum, inexpensive, non-toxic, readily biodegradable, having a high viscosity, and being hydrophilic [6-8]. In addition, PVA does not cause lattice mismatch or flaws at the nanocrystal/capping matrix interface [9]. Several authors have previously shown that semiconductor nano crystals topped with PVA have improved physical

International journal of basic and applied research
www.pragatipublication.com
ISSN 2249-3352 (P) 2278-0505 (E)
Cosmos Impact Factor-5.86

characteristics [10,11]. Previous research has also shown that solar cells made using a variety of semiconductors and covered with PVA as an absorber layer have high conversion efficiency [12]. One set of semiconductors that has shown promise as an absorber layer for solar cell applications is SnS, which belongs to the IV-VI group. Reasons for this include SnS's p-type conductivity, cheap cost, abundance of elements on Earth, high hole mobility, low toxicity, and direct optical band gap of 1.3 eV, among other desirable features [13–18]. In most cases, the distinctive characteristics of nanomaterials make them more important than bulk materials. A literature search turned up many studies discussing the production of SnS nanoparticles [19]. In the past, many physical and chemical techniques were used to create SnS films. These included thermal evaporation [23,24], chemical bath deposition [20-22], RF sputtering [25,26], spray pyrolysis [27,28], and electron beam evaporation [29]. We grew PVA-capped SnS nanocrystalline layers at varying concentrations using the chemical bath deposition approach in this study. The simplicity, low processing temperature, and affordability of the current technology were the deciding factors. For the first time, this study studies, analyses, and reports on the effects of PVA concentration on PVA-capped SnS layers; no other work on SnS has done this.

3. EXPERIMENTAL DETAILS

3.1. Reagents

In this work, stannous chloride ($SnCl_2$,$2H_2O$) and thioacetamide (C_2H_5NS) were used as precursors for tin and sulphur, tartaric acid ($C_4H_6O_6$) as a complexing agent and polyvinyl alcohol $(-CH_2CHOH-)_n$ (average M.W.=1,60,000) as a capping agent to prepare PVA capped SnS layers.

3.2. Method

Nanocrystalline SnS films were synthesized on glass substrates using chemical bath deposition at four different PVA concentrations varying in the range, 0.5 – 2 wt %. Initially, double distilled water was used to prepare solutions of 0.1 M stannous chloride ($SnCl_2$, $2H_2O$), 0.2 M thioacetamide (C_2H_5NS) and 0.5 M tartaric acid. PVA solutions at different concentrations were prepared using the following procedure. Different wt % of PVA solutions were taken in a glass beaker and then stirred at a temperature of 80 ^oC using a magnetic stirrer. The process should be continued until getting a transparent solution and then the solution was allowed to cool to room temperature. Now, 50 ml of PVA solution of particular concentration, 20 ml of stannous chloride and 10 ml of tartaric acid were taken in a beaker and placed on a magnetic stirrer to stir well. 20 ml of thioacetamide was added to this solution and continued to stir the mixture in the beaker. Cleaned glass substrates were vertically immersed into the reaction bath and continued to stir the solution by maintaining a constant bath temperature of 80 ^oC with a fixed deposition time of 90 minutes. Finally, the deposited films were cleaned using double distilled water and dried in a hot air oven. Light brown colour solution at the beginning was turned into dark brown at the final stage of film deposition.

The structural properties of the synthesized PVA capped SnS films were studied by Bruker (D8 Advance) X-ray diffractometer, using CuKα (λ = 1.5408 Å) radiation. DIPOLAR XY 800 Raman spectrometer was used to record Raman spectra in the backscattering configuration at the room temperature with unpolarized light. The SEM micrographs were undertaken to study surface morphology using Carl Zeiss EVO 50 scanning electron microscope (SEM). Park NX10 AFM atomic force microscope (AFM) was used to investigate the grain size and the surface

International journal of basic and applied research
www.pragatipublication.com
ISSN 2249-3352 (P) 2278-0505 (E)
Cosmos Impact Factor-5.86

roughness of the films. FTIR spectra were recorded using Thermo Nicolet FTIR spectrophotometer. Optical measurements were carried out using JASCOV-770 UV-VIS-NIR

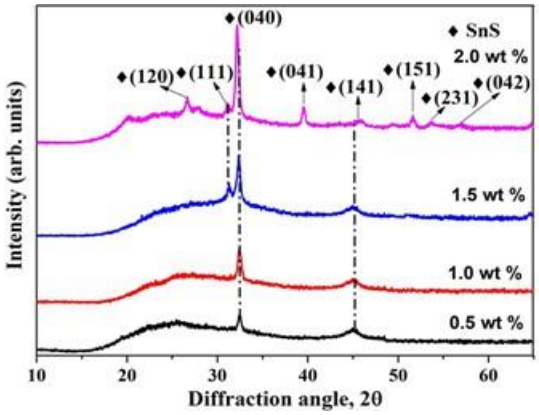

double beam spectrophotometer. ECOPIA HMS 5000 Hall measurement system was used for electrical characterization.

4. RESULTS AND DISCUSSIONS

The deposited PVA capped SnS layers appeared dark brown in colour, homogeneous without the presence of any voids and pinholes.

4.1. Structural analysis

4.1.1. XRD analysis

X-ray diffraction patterns of PVA capped SnS layers deposited at four different PVA concentrations that varied in the range of 0.5 - 2 wt % are shown in Fig. 1. The XRD spectra exhibited many peaks oriented in different directions confirmed the polycrystalline nature of all the deposited films. All the films had the (040) peak with high intensity observed at 2θ= 32.0° compared to other reflections that correspond to the orthorhombic crystal structure. Along with the predominant peak, the XRD spectra exhibited various other peaks, particularly for the layer deposited at 2 wt % concentration of PVA. These peaks were observed at 2θ= 26.02°, 31.50°, 39.40°, 44.88°, 51.42°, 53.89° and 56.73° that corresponds to (120), (111), (040), (041), (141), (151), (231) and (042) planes of SnS, which matched closely with the data reported in JCPDS card no. 39-0354. It is noticed that the PVA capped SnS layers do not contain any secondary phases of SnS such as Sn_2S_3 and SnS_2. On the other hand, the films deposited upto 1.5 wt % of PVA concentration showed different low intensity peaks, which might be because of low crystallinity in the films. The increase in intensity of the predominant peak with the increase in PVA concentration indicates betterment in the crystallinity of the films.

Thus good quality SnS films can be observed for the layers deposited at 2 wt % of PVA concentration, might be suitable for the device applications.

Fig. 1. X-ray diffraction patterns of PVA capped SnS films grown at different PVA concentrations.

The variation of crystallite size, lattice strain, dislocation density and stacking faults with PVA concentration was determined and plotted in Fig. 2. The average crystallite size (D) of

International journal of basic and applied research
www.pragatipublication.com
ISSN 2249-3352 (P) 2278-0505 (E)
Cosmos Impact Factor-5.86

PVA capped SnS layers had been evaluated using the following Debye-Scherrer formula [30],

$$D = \frac{K\lambda}{\beta \cos\theta} \text{ (nm)} \qquad (1)$$

where K is equal to 0.94, called as the shape factor and β is the full width at half maximum of the predominant peak. The estimated values of average crystallite size were varied in the range, 9 – 22 nm with the variation of PVA concentration from 0.5 wt % to 2 wt %. Thus, there is an increase in the values of crystallite size with PVA concentration. This result indicated that there was an increase in the nucleation of ad-atoms on the substrate surface with increase of PVA concentration.

The number of dislocations per unit volume can be determined using the following relation [31],

$$\delta = \frac{1}{D^2}$$

The evaluated values of dislocation density with PVA concentration were varied in the range, 12 – 2 lines / m^2. The decrease in dislocation density with PVA concentration indicated an improvement in the quality of the deposited layer. Hence, the layers deposited at 2 wt % of PVA concentration with low dislocation density lead to decrease the imperfections and increase the layer crystallinity.

The mismatch of lattice between the PVA capped SnS layers and the substrate can be measured using lattice strain (ε), determined using the following relation [32],

$$\varepsilon = \frac{\beta}{4\tan\theta}$$

where the symbols have usual meaning. It is noticed that the value of lattice strain was decreased with the increase of PVA concentration and varied in the range, 13.5 x 10^{-2} - 5.9 x 10^{-3}. The value of lattice strain is more for the layers deposited at lower PVA concentration that is mainly because of the presence of defects and imperfections, which in turn decreases for further rise of PVA concentration to 2 wt %.

International journal of basic and applied research
www.pragatipublication.com
ISSN 2249-3352 (P) 2278-0505 (E)
Cosmos Impact Factor-5.86

The periodic sequence of atomic planes can be altered due to a planar defect, named as stacking faults developed during growth of crystallographic planes in the deposited layers. The following relation [33] was used to determine stacking faults,

The evaluated values of stacking faults were decreased with the increase of PVA concentration and varied in the range, 7.4 x 10^{-3} – 3.2 x 10^{-3}. Therefore, similar to dislocation density and lattice strain, the value of stacking faults also low for the layer deposited at 2 wt % of PVA concentration relative to other layers.

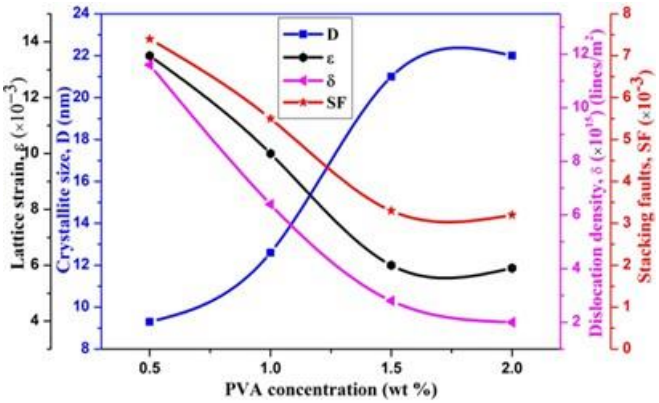

Fig. 2. Variation of lattice strain, crystallite size, dislocation density and stacking faults with PVA concentration (wt %).

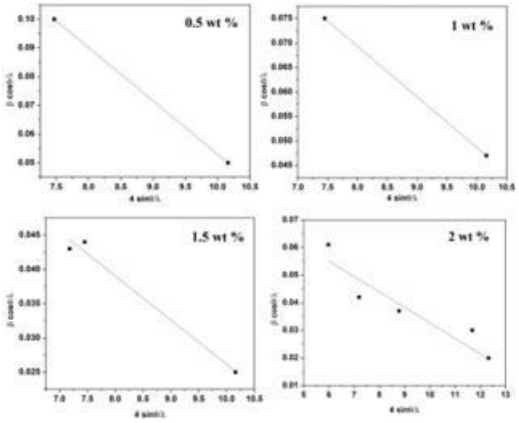

Fig. 3. W-H plots of PVA capped SnS layers at different PVA concentrations.

The average crystallite size can also be estimated using Williamson-Hall plots. This method involved the usage of many crystal planes from the XRD spectrum in the calculation of crystallite size rather than only the prominent peak used in Scherrer's formula. Fig. 3 shows Williamson – Hall plots for the experimental films grown in this work. The estimated average crystallite size using W-H plots were varied from 4 nm to 12 nm with the variation of PVA concentration from 0.5 wt % to 1 wt %.

International journal of basic and applied research
www.pragatipublication.com
ISSN 2249-3352 (P) 2278-0505 (E)
Cosmos Impact Factor-5.86

4.1.2. Raman analysis

Fig. 4 shows the Raman spectra of PVA capped SnS layers deposited at various concentrations of PVA that varied in the range from 0.5 wt % to 2 wt %. The spectra exhibited a strong Raman mode belongs to tin mono sulphide (SnS) appeared at 94 cm^{-1} for all the deposited layers. In addition to this strong mode, the layers had two other modes appeared at 166 cm^{-1}, 219 cm^{-1}. All the observed Raman modes were related to SnS phase with orthorhombic structure. Also, these modes were matched with the reported data on SnS [34-36]. Similar to XRD spectra, Raman spectra also does not show any secondary phases of Sn and S such as SnS_2 and Sn_2S_3. The Raman modes appeared at 94 cm^{-1} and 219 cm^{-1} belongs to A_g [36] mode and the mode at 166 cm^{-1} represents B_{3g} [37]. Furthermore, the intensity of Raman modes were highly influenced by the PVA concentration in such a way that the intensity increases with increase of concentration of PVA for all the observed modes. This clearly indicates that there is an improvement in the crystallinity of the layers with PVA concentration. This result is in agreement with the XRD analysis discussed earlier.

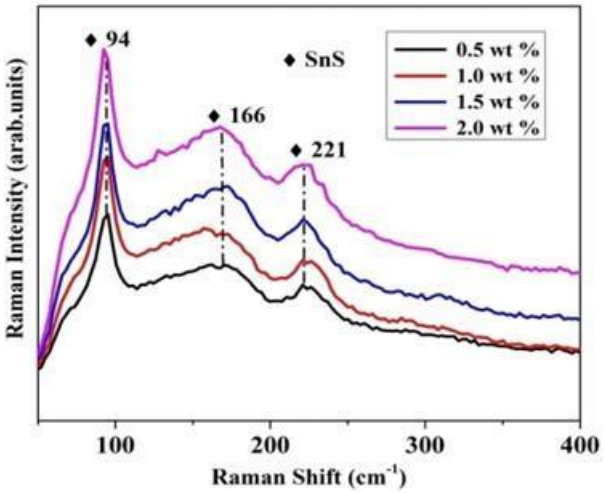

Fig. 4. Raman spectra of PVA capped SnS layers grown atdifferent PVA concentrations.

4.2. Surface morphology

4.2.1. Morphological studies

The surface morphology of PVA capped SnS films deposited at different PVA concentrations was studied using scanning electron microscopy (SEM) and the corresponding micrographs are shown in Fig. 5. The SEM micrographs of SnS films grown at 0.5 wt % and 1 wt % concentrations of PVA contains poor morphology with very few gains of different shapes present. With the increase of PVA concentration to 1.5 wt %, there is an improvement in the surface morphology with the development of grains. Finally, the films deposited at 2 wt % of PVA concentration showed a greater number of large sized grains. This clearly indicates that higher PVA concentration can effectively increase the crystallinity, regulate the shape of the grown SnS nanocrystals and also controls the crystallite size.

International journal of basic and applied research
www.pragatipublication.com
ISSN 2249-3352 (P) 2278-0505 (E)
Cosmos Impact Factor-5.86

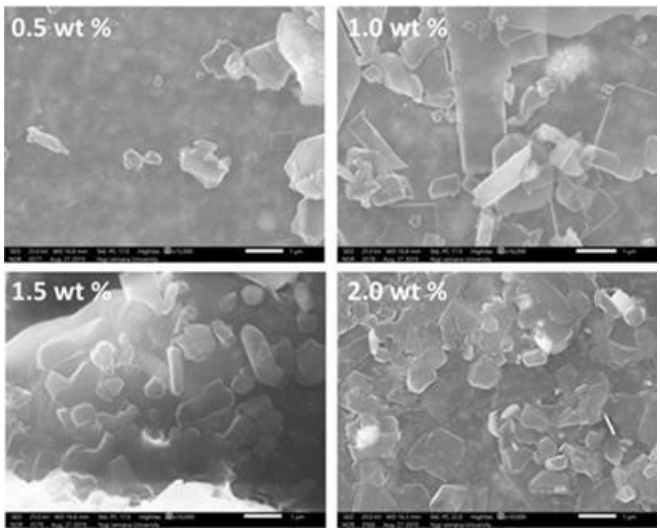

Fig. 5. SEM images of PVA capped SnS layers deposited at different PVA concentrations.

4.2.2. Topographical analysis

Fig. 6 shows the 3-dimensional AFM images of PVA capped SnS layers deposited at four different PVA concentrations that varied in the range, 0.5 - 2 wt %. The images clearly indicated that the grain growth was influenced mainly by the PVA concentration. For the layers deposited at 0.5 wt % and 1 wt % PVA concentration, few crystallites grew with small size similar to the SEM result. With the increase of PVA concentration to 1.5 wt %, the crystallite size also increased and grew in irregular shape. For further rise of PVA concentration to 2 wt %, the layers had bigger crystallites without the presence of any voids. This might be because of the fact of existence of second nucleation for the layers deposited at 2 wt% concentration of PVA and therefore bigger sized crystallites are formed due to the joining of all ad-atoms over the surface of the substrate. This clearly indicates that there is an improvement in the crystallinity of the layers with PVA concentration. The average crystallite size was increased with PVA concentration and varied in the range, 5.6 – 10.2 nm. Also, a small change of the surface roughness with increase in PVA concentration was observed from the AFM images. Thus, the layers deposited at 2 wt % of PVA concentration, showed high crystallinity and smooth surface, might be suitable for device applications.

International journal of basic and applied research
www.pragatipublication.com
ISSN 2249-3352 (P) 2278-0505 (E)
Cosmos Impact Factor-5.86

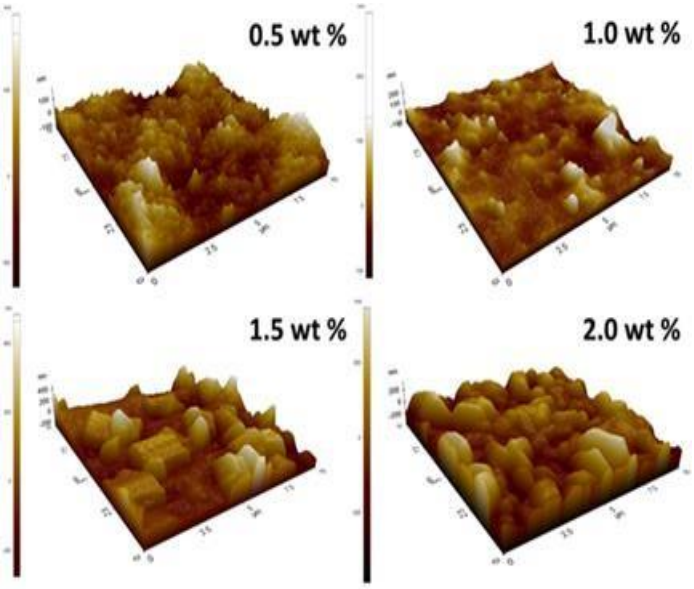

Fig. 6. AFM pictures of PVA capped SnS layers grown at different PVA concentrations.

4.3. FTIR analysis

Fig. 7 represents the Fourier transform infrared spectra of PVA capped SnS nanocrystals deposited using different PVA concentrations that varied in the range, 0.5 – 2 wt %. This analysis was undertaken in order to determine the presence of PVA and SnS in the experimental films. The characteristic FTIR band spectra clearly indicated that the layers deposited at 0.5 wt % of PVA concentration contained lot of noise with the absence of sharp bands. As already discussed earlier, the layer with 0.5 wt % of PVA concentration does not contain the sufficient PVA concentration for the proper growth of SnS nanocrystals. On the other hand, the remaining layers formed at different PVA concentrations (≥1 wt %) showed various absorption bands of both PVA and SnS. The band observed at 3757 cm^{-1} corresponding to the O-H stretching vibration of hydroxyl groups of PVA. The CH_2 asymmetric stretching vibration belongs to the band at 2938 cm^{-1}. The bands observed at 1707 cm^{-1}, 1518 $cm^{-1}$and 1030 cm^{-1} were assigned to C=C stretching vibration, C-H bending vibration and C-O stretching of acetyl groups present in PVA. The band observed at 839 cm^{-1} was assigned to C-C stretching vibration. The bands observed at 2355 cm^{-1} [38]. This analysis clearly proves the presence of PVA in SnS nanocrystalline layers.

International journal of basic and applied research
www.pragatipublication.com
ISSN 2249-3352 (P) 2278-0505 (E)
Cosmos Impact Factor-5.86

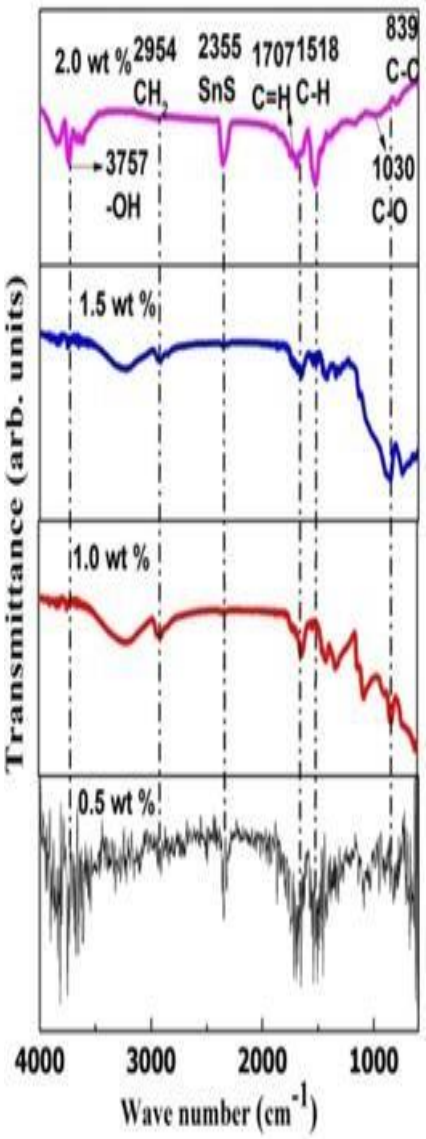

Fig. 7. FTIR spectra of PVA capped SnS layers grown at different PVA.

4.4. Optical analysis

Fig. 8 represents the optical transmittance and reflectance spectra of PVA capped SnS layers formed using four different PVA concentrations that varied from 0.5 wt % to 2 wt %. In the visible range, all the deposited layers had shown lower values of both transmittance (T) and reflectance (R) that might indicate high light absorption in this region. Also, transmittance and reflectance decreased with increase of PVA concentration. Further the fall of transmittance with wavelength near the fundamental absorption edge is slow indicating low crystallinity of the synthesized layers. Thus, the layer deposited at 2 wt % of PVA concentration had shown the highest absorption of light compared to the other layers.

International journal of basic and applied research
www.pragatipublication.com
ISSN 2249-3352 (P) 2278-0505 (E)
Cosmos Impact Factor-5.86

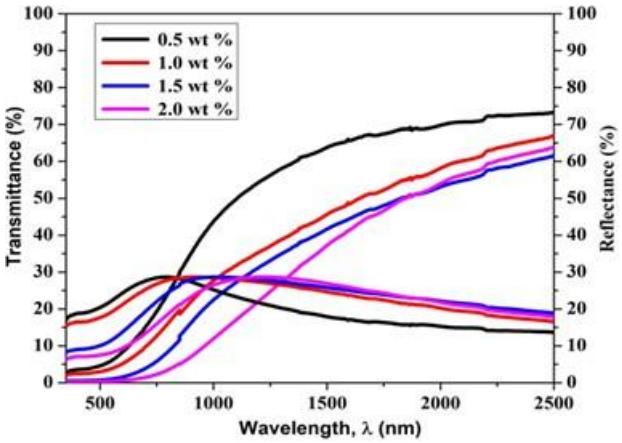

Fig. 8. Optical transmittance and reflectance spectra of PVA capped SnS layers.

The Lambert's relation [39] was used to determine optical absorption coefficient (α) values of SnS layers. The film thickness used for calculating the absorption coefficient was approximately 150 nm, as determined from the SEM cross-section of the film. The estimated values of α were plotted against photon energy for all the deposited layers and are given in figure 9. It can be seen from the figure that the optical absorption coefficient is $>10^5$ cm^{-1} for the all the deposited layers. Moreover, the layers deposited at 2 wt % of PVA concentration had very high value of the absorption coefficient compared to other layers, which might be due to the increase of crystallinity of the layers and therefore such layers might be suitable for solar cells application as an absorber layer. Further, the observed increase of absorption coefficient with the rise of PVA concentration is also supported by the low values of transmittance and reflectance noticed for the corresponding layers that can be seen from Fig. 9.

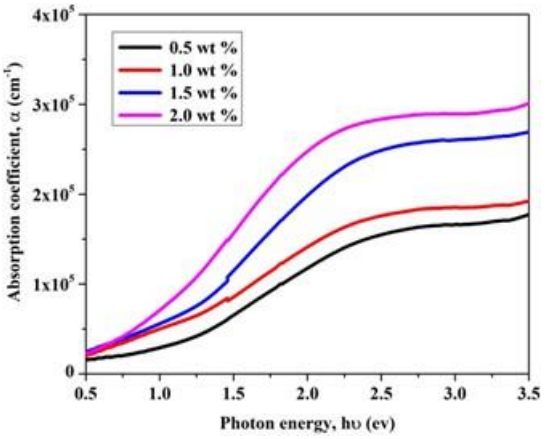

Fig. 9. Variation of absorption coefficient with photon energy.

The following mathematical relation was used to estimate the optical energy band gap values of PVA capped SnS films [40],

$$\alpha h\upsilon = A(h\upsilon - E_g)^{1/2}\,(\text{eV/cm}) \qquad (5)$$

where hυ is photon energy and A is constant. In the present work, Tauc plots were drawn for all the deposited layers and are indicated in Fig. 10.

International journal of basic and applied research
www.pragatipublication.com
ISSN 2249-3352 (P) 2278-0505 (E)
Cosmos Impact Factor-5.86

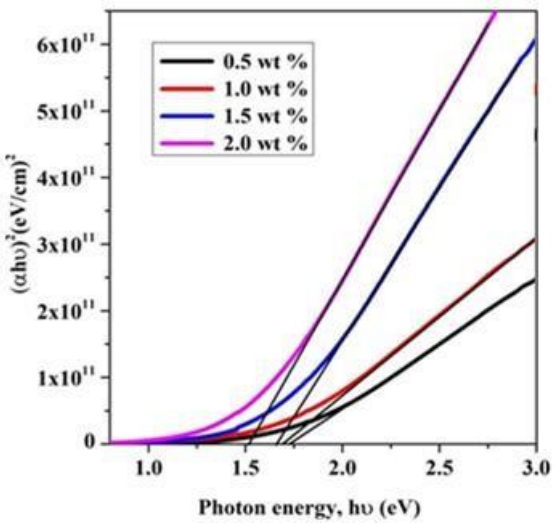

Fig. 10. Tauc plots of PVA capped SnS layers grown atdifferent PVA concentrations.

The optical energy band gap values were evaluated from the intercept of linear portion of the plots and found to vary in the range, 1.73 - 1.53 eV with increase of PVA concentration. Thus, the band gap value decreases with the increase of PVA concentration. Also, this result of blue shift in the band gap values compared to bulk SnS was attributed to quantum confinement in the experimental films. Brus equation [41], given below, was used to estimate the particle size.

$$h^2 \left[\frac{1}{} \quad \frac{1}{} \right] 1.8e^2$$

where E_n is the band gap value of observed SnS layers, E_g is the energy band gap of bulk SnS (~1.3 eV), m_h^* (= 0.109 m_0) and m_e^* (= 0.5 m_0) [42] are the effective masses of hole and electron of SnS and ε is the dielectric constant of SnS and is taken as 12.4 [43]. The particle size values of PVA capped SnS layers estimated using the above relation varied slightly from 6.2 nm to 8.8 nm with the increase of PVA concentration.

4.5. Electrical Properties

Hall effect measurements were under taken to study the electrical properties of PVA capped SnS layers deposited at different PVA concentrations. The studies showed a positive Hall coefficient for all the prepared layers, indicating that all the experimental layers had p-type electrical conductivity. The variation of electrical resistivity (ρ), Hall mobility (μ) and carrier concentration (N) of PVA capped SnS layers with various PVA concentrations, varying from 0.5 wt % to 2 wt % is shown in Fig. 11.

International journal of basic and applied research
www.pragatipublication.com
ISSN 2249-3352 (P) 2278-0505 (E)
Cosmos Impact Factor-5.86

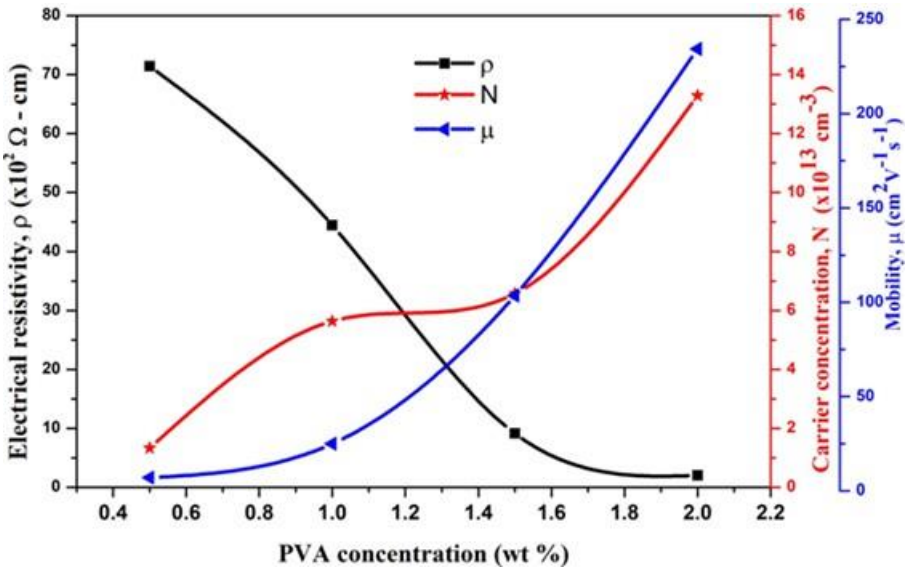

Fig. 11. Variation of electrical parameters with PVA concentration.

From the figure, it is noticed that the PVA concentration significantly influenced the electrical resistivity, carrier mobility and carrier concentration. The measured electrical resistivity values decreased with the increase of PVA concentration from 0.5 wt % to 2 wt %. The reason for this decrease in electrical resistivity might be due to the fact of decrease in grain boundary area with the increase in PVA concentration, which in turn decreases the scattering of the carriers at the grain boundaries. Also, the carrier mobility of the films increased with the increase of PVA concentration. Furthermore, from the graph, it is noticed that the carrier concentration increased with the increase of PVA concentration. The increase of carrier concentration and also carrier mobility with PVA concentration is mainly because of the increase in packing density. Thus the layers deposited at a PVA concentration of 2 wt % might be suitable as an absorber layer in solar cell devices as it had high carrier mobility and low resistivity.

5. CONCLUSIONS

Using a basic chemical bath approach, the first ever effective deposition of PVA-capped SnS nanocrystalline layers on glass substrates was achieved, with PVA concentrations ranging from 0.5 to 2 weight percent. The deposited films are nanocrystalline, according to the XRD spectra, which also showed a single SnS phase with a sharp peak at the (040) plane. The range of the estimated average crystallite size was 4 nm to 12 nm, and it rose as the PVA concentration rose. The phonon modes corresponding to the SnS phase were revealed by the Raman analysis, which is in accordance with the XRD findings. Micrographs taken with scanning electron microscopes and atomic force microscopes revealed large crystals and a smooth surface morphology on the layers deposited with a 2 wt% PVA concentration. Grain sizes ranged from 5.6 nm to 10.2 nm, according to AFM measurements. The FTIR spectra of the SnS nanocrystalline layers verified that PVA was present. The optical tests revealed that each layer had an exceptionally high optical absorption coefficient, approximately equal to 105 cm-1. Optical band gap values measured using Tauc plots ranged from 1.73 eV to 1.53 eV as the concentration of PVA increased. Particle sizes ranged from 6.2 nm to 8.8 nm, according to optical examinations. Hall tests verified that all of the PVA-coated SnS films were p-type.

The electrical resistivity decreased while the mobility and carrier concentration increased with increase of PVA concentration. Hence, the layers deposited at 2 wt % of PVA concentration had better structural, morphological, optical and electrical properties and might be suitable as an absorber layer in solar cell development.

REFERENCES

Microelectronic Engineering, 183–184, 2007, 48–51, by T. Ghomian, S. Farimand, and J. W. Choi, explored the impact of isopropylamine-capped PbS quantum dots on infrared photodetectors and photovoltaics.
[2] PbS/polyvinyl alcohol nanocomposites for flexible high dielectric thin film applications: growth and properties, Thin Solid Films, 598, 2016, 243-251, J.J.L. Hmar, T. Majumder, and S.P. Mondal.
[3] In a 2014 study published in the Journal of Material Science: Materials in Electronics, I.S. Elashmawi, A.M. Abdelghany, and N.A. Hakeema discuss the quantum confinement effects of CdS nanoparticles scattered inside PVP/PVA nanocomposites (24, 2956-2961).
The optical and electrical characteristics of sol-gel produced CdS nanoparticles doped with polyvinyl alcohol were studied by M. Sharma and S.K. Tripathi in their 2015 work published in the Journal of Material Science: Materials in Electronics, volume 26, pages 2760–2768.
[5] X-ray diffraction line profile characterization of polyvinyl alcohol capped cadmium sulphide nanostructured films authored by P K. Mochahari and K C. Sarma was published in the Indian Journal of Physics in 2014 and can be found on pages 1265-1270.
The function of the host polymer matrix in the light emission processes of a nano-CdS/polyvinyl alcohol composite, by G. Yu. Rudko, A. O. Kovalchuk, V. I. Fediv, O. Ren, W. M. Chen, I. A. Buyanova, and G. Pozina, [6] Chapters 11–15 of Thin Solid Films, volume 543, published in 2013.
A. A. Shabaka, S. Abd EI Mongy, and R. Seoudi, Research on the influence of polyvinyl alcohol matrices on spectroscopic and structural investigations of CdSe nanoparticles, published in Physica B: Condensed Matter in 2008, pages 1781–1786.
[8] Prem Ajibade and J. Osuntokun Nanoparticles of zinc and cadmium sulfide in a polyvinyl alcohol matrix: morphological and thermal investigations, Physica B: Condensed Matter, 496, 2016, 106–112.
S. N. Sahu and J. Nayak Optical characteristics and structure of GaAs nanocrystals capped with polyvinyl alcohol, Physica E: Low Dimensional Systems and Nanostructures, 30, 2005, 107-113.
[10] As stated in Optik 127, 2016, 2586-2589, K. S. Ojha examined the optical and structural characteristics of thin films of zinc sulfide doped with PVA.
[11] G. Kortaberria, A. Tercjak, H. Etxeberria, J. Gutierrez, and I. Barandiaran Changing the capping agent to tune the photoresponsive and dielectric characteristics of PVA/CdSe films, Composites Part A: Applied Science and Manufacturing, 118, 2019, 194-201.
Saikia, D., and Phukan, P. [12] Thin Solid Films, 562, 2014, 239-243, describes the chemical bath deposition method for fabricating and evaluating CdS/PbS thin film solar cells.
[13] In the Journal of Physics: Condensed Matter, Longfei Pan, Shuhao Yuan, Jiahong Lin, Bingsuo Zou, and Li-Jie Shi discuss the adjustable bandgap effect of SnS films in their 2018 article 465302.
C-C. Huang, Y-J. Lin, C-J. Liu, and Y-W. Yang, on page fourteen, Microelectronic Engineering, 110, 2013, 21–24, discusses the photovoltaic characteristics of n-type SnS contacts on unpolished p-type Si surfaces with and without sulfur treatment.
(Reddy, K. T. Ramakrishna, Reddy, N. Koteswsara, and R.W. Miles) Solar Energy Materials and Solar Cells, 90(6), 3041-3046, 2006, discusses the photovoltaic characteristics of solar cells based on SnS.
The impact of deposition duration on the electrical, optical, structural, and mechanical characteristics of SnS thin films created by chemical bath deposition was studied by Guneri et al. (2010) in the journal Applied Surface Science, volume 257, pages 1189–1195.

"Impact of growth temperature on the properties of SnS films prepared by thermal evaporation and its photovoltaic performance" (Current Applied Physics, 15, 2015, 897-901), written by Y. Kawano, J.

International journal of basic and applied research
www.pragatipublication.com
ISSN 2249-3352 (P) 2278-0505 (E)
Cosmos Impact Factor-5.86

Chantana, and T. Minemoto.
[18] In the Journal of Physics: Conference Series, 682, 2016, 012019, M. Ganchev, P. Vitanvov, M. Sendova-Vassileva, G. Popkirov, and H. Dikov discuss the characteristics of SnS thin films produced via physical vapour deposition.
Growth and photovoltaic performance of SnS quantum dots, by K. G. Deepa and J. Nagaraju, Materials Science and Engineering B, 17, 2012, 1023-1028.
Evaluation of the influence of pH and deposition methods on tin sulphide thin films produced by chemical bath deposition, by A. Higareda-Sanchez, R. Mis-Fernandez, I. Rimmaudo, E. Camacho-Espinosa, and J.L. Pena, published in Superlattices and Mirostructures in 2021 and with the DOI number 106831.
The authors of the cited work are Jing, Cao, Huang, Lai, Sun, Wang, and Shen [21]. Journal of Alloys and Compounds, 726, 2017, 720-728, describes chemical bath deposition of SnS nanosheet thin films for FTO/SnS/CdS/Pt photocathode.
[22] In the International Journal of Hydrogen Energy, Sergio Battiato et al. discuss the use of composition-controlled chemical bath deposition of Fe-doped NiO microflowers to enhance oxygen evolution reaction. The study was published in 2023 and can be found on pages 18291–18300.
[23] In Optik, 244, 2021, 167460, R. Balakarthikeyen et al. analyze the performance of SnS thin films made using the thermal evaporation approach for use as photodetectors. The authors include A. Santhanan, Aslam Khan, Ahmed M.EI. Toni, A. Anees, Ansari, Ahmamad Imran, Mohd. Shkir, and S. AlFaify.
[24] In Thin Solid Films, 639, 2017, 7-11, K.O. Haraa, S. Suzuki, and N. Usami discuss the creation of a metastable cubic phase in SnS thin films made by thermal evaporation.
Journal of Alloys and Compounds, 831, 2020, 154626, S-IK. Son et al., Effect of working pressure on the characteristics of RF sputtered SnS thin films and photovoltaic performance of SnS-based solar cells [25] (Y. Guk Son, C. Sik Son, D. Ryeol Kim, J. Hyung Park, S. Kim, D. Hwang, and P. Song).
[26] In Thin Solid Films, K. Hartman et al. (2011) presented SnS thin films produced by radiofrequency sputtering at ambient temperature (Thin Solid Films, 519, 2011, 7421–7424).
A study conducted by Y. Nouri, B. Hartiti, H. Labrim, A. Ziti, A. Belfhaili, A. Batan, S. Fadili, Mounia, Tahri, and P. Thevenin was published in Optical Materials in 2022 and covers the synthesis of tin monosulfide SnS thin films using a spray pyrolysis process based on a Taguchi design for solar absorbers.
Reference: [28] Andrade-Arvizu, J. A., Garcia-Sanchez, M. F., Courel-Piedrahita, M., Agudelo, P., Santiago-Jaimes, E., Valecia-Resendiz, A., Arce-Piaza, and Galán, O. Optimal growth conditions, including conversion types of conductivity, on SnS thin films produced by chemical spray pyrolysis, Journal of Analytical and Applied Pyrolysis, 121, 2016, 347-359.
[29]The optical and photoconductive characteristics of SnS thin films generated by electron beam evaporation were studied by A. Tanusevski and D. Poelman in Solar Energy Material and Solar Cells, volume 80, issue 3, 2003, pages 297–303.
N. S. Saenko published an article in Physics Procedia in 2012 titled "The X-ray diffraction study of three-dimensional disordered network of nanographites: experiment and theory" (23, 102–105).
In their work, A. Purohit, S. Chander, S.P. Nehra, and M.S. Dhaka [31] Physica E: Low Dimensional Systems and Nanostructures, 69, 2015, 342-348, discusses the impact of air annealing on the electrical, structural, optical, and morphological characteristics of CdSe thin films that have been thermally evaporated.
In a study published in 2017 in Materials Science in Semiconductor Processing, the authors [32] examined the optical characteristics of In2S3 thin films that had been thermally evaporated and measured using photoacoustic spectroscopy. The results showed interesting findings.

T. Sreenivasulu Reddy, G. Phaneendra Reddy, and K.T. Ramakrishna Reddy assessed the electrical and optical characteristics of conductive and transparent MO-doped ZnO films by varying the concentration of

MO, [33] Published in 2018, volume 458, pages 333–343.
[34] In the Journal of Molecular Structure, 1152, 2018, 137–144, A.M.S. Arulanantham et al. discuss the use of nebulizer spray pyrolysis (NSP) to create SnS thin films including FTO, CdS, and SnS for use in solar cells.
Liquid-phase deposition of thin films of tin monosulfide (SnS) was described in a 2017 article by S. Banu, S. Jin Ahn, Y. JooEo, J. Gwak, and A. Cho in Sol Energy, volume 145, pages 33–41.
Thin films of SnS produced by chemical spray pyrolysis at varying substrate temperatures for use in photovoltaics, by T. Sall, B.M. Soucase, M. Mollar, and J.A. Sans, published in the Journal of Electronic Materials in 2017, pages 1714–1719.
[37] In the 2017-012007 issue of the IOP conference series on materials science and engineering, S. Ali, F. Wang, S. Zafar, and T. Iqbal discuss the hydrothermal synthesis, characterization, and Raman vibrations of chalcogenide SnS nanorods.
Das, D., and Dutta, R. Kumar [38] Journal of Colloid and Interface Science, 457 (2015), 339-344, describes a new way to make SnS nanorods with a narrow band gap and how they degrade dyes efficiently via photocatalysis.
SnS layers produced by chemical bath deposition: comprehensive optical investigations (G. Sreedevi, M. Vasudeva Reddy, C. Park, J. Chan-Wook, and K.T. Ramakrishna Reddy, 2015, Optical Materials, 42, 468-475).
The development of sulphurized SnS thin film solar cells was published in Current Applied Physics in 2015 and was co-authored by M.R. Vasudeva Reddy, G. Sreedevi, C. Park, R.W. Miles, and K.T. Ramakrishna Reddy. The article can be found on pages 588-598.
The article "Electronic Electronic Wave Functions in Semiconductor Clusters: Experiment and Theory" by L. Brus was published in The Journal of Physical Chemistry in 1986 and can be found on pages 2555-2560.
[42] Article cited as "Strong quantum confinement effects in SnS nanocrystals produced by ultrasound-assisted method" in the Journal of Nanoparticle Research (volume 15, issue 13, 2013) by Y. Azizian-Kalandaragh, A. Khodayari, Z. Zeng, C.S. Garoufails, S. Baskoutas, and L.C. Gontard.
Report on numerical study of SnS heterojunction performance (J. Xu and Y. Yang, 2014, pp. 260–265) published in Energy Conversion and Management.